

## MixPI: User Guide

Britta A. Johnson,<sup>1</sup> Siyu Bu,<sup>2</sup> Gregory Schenter,<sup>1</sup> Christopher J. Mundy,<sup>1</sup> and Nandini Ananth<sup>2</sup>

<sup>1</sup>*Physical Science Division, Pacific Northwest National Laboratory, Richland, Washington 99352, USA*

<sup>2</sup>*Department of Chemistry and Chemical Biology, Cornell University, Ithaca, New York 14850, USA*

(Dated: 2 December 2024)

## I. FUNDING ACKNOWLEDGEMENT

B.A.J., C.J.M., and G.S. acknowledge current support by the DOE Office of Science, Office of Basic Energy Sciences, Division of Chemical Sciences, Geosciences, and Biosciences, Condensed Phase and Interfacial Molecular Science program. N.A. and B.A.J. acknowledge support from the U.S. Department of Energy, Office of Basic Energy Sciences, Division of Chemical Sciences, Geosciences and Biosciences under Award DE-FG02-12ER16362 (Nanoporous Materials Genome: Methods and Software to Optimize Gas Storage, Separations, and Catalysis). S.B. acknowledges support from Cornell University, Department of Chemistry and Chemical Biology.

## II. DOWNLOADING AND COMPILING MIXPI

### A. Download

#### 1. *MixPI*

The most recent version of MixPI is v1.0. Subsequent versions will be developed and updated to this page. The following subdirectories are located within the MixPI download:

- `src/` : Contains the source codes for MixPI.
- `examples/` : Example input files for a MTS bulk water simulation and a  $\text{Co}^{3+} + e^-$  simulation
- `updated-cp2k-files/` : The cp2k source files that were updated to interface with MixPI

All files in the `src/` folder should be downloaded. Files that contain the changes to CP2K are also located in the `updated-cp2k-files/` and need to be downloaded as well.

#### 2. *CP2K*

MixPI requires the installation of the molecular dynamics package CP2K v2023.2<sup>1</sup> which can be found on the CP2K website. CP2K must be installed as both an executable and library. The instructions for each are also located on the CP2K website. A few changes to

the CP2K source code were made in the development of MixPI. These changes were made to the following CP2K files:

- `constraint.F`
- `constraint_vsite.F`
- `start/libcp2k.F`
- `subsys/molecule_kind_types.F`
- `topology_connectivity_util.F`
- `topology_coordinate_util.F`
- `topology_generate_util.F`
- `topology_psf.F`
- `topology_types.F`
- `topology_util.F`

Unless indicated, these files are located in the `src/` directory. The updated versions of these files are located in the MixPI directory `updated-cp2k-files/`. These changes do not interfere with running CP2K as normal.

## B. Compile

### 1. *CP2K*

After replacing the updated files in the `src/` directory; the authors suggestion using the toolchain build to generate arch files and compile CP2K. The instructions below will assume the toolchain was used. Instructions for the toolchain build are found in the CP2K documentation. To build the CP2K version used by the authors, the following steps were used.

- From the `cp2k/` directory, access the toolchain and run the install command. `cd /tools/toolchain/`

`./install_cp2k_toolchain.sh`

For additional features to be linked to CP2K (like PLUMED), include those in the install line. (For example `./install_cp2k_toolchain.sh - -with-plumed` )

- After build, copy the arch files generated in `install/arch` to the `cp2k arch` directory  
`cp install/arch/local* ../../arch/`

- Source the locations of the libraries that are linked to CP2K  
`source install/setup`

- Return to the `cp2k` directory and compile.

`cd ../../`

`make -j 12 ARCH=local VERSION='ssmp sdbg ssmp pdbg'`

- After successful compilation, compile `cp2k` as library.

`make -j 12 ARCH=local VERSION='ssmp sdbg ssmp pdbg' libcp2k`

## 2. *MixPI*

After compiling CP2K as an executable and library, the paths in the makefile for MixPI must be updated to find the correct libraries. This is done with three separate updates:

- Copy all libraries flags from the CP2K arch file (The arch file is `arch/local.psm` and the `-l***` flags are located following `"LIBS="`.) onto the `"LIB ="` line in the makefile located in the `src/` directory of MixPI. (To find these libraries, updated the `-I` and `-L` paths within the makefile or, if compiled with the toolchain build, source the same setup file as used when building `cp2k`.)

- Update the locations of the `cp2k/dbcsr` libraries and object files. They are located at:

`CP2K_LIB = /**cp2k-directory**/lib/local/psmp`

`DBSCR_LIB = /**cp2k-directory**/lib/local/psmp/objs/dbcsr`

```
CP2K_INC = /**cp2k-directory**/obj/local/psmp
DBSCR_INC = /**cp2k-directory**/obj/local/psmp/exts/dbcsr
```

This should generate an executable (cp2k\_pimd.out) which will run MixPI.

### III. INPUT

In this section, we introduce the specific input files needed to run the MixPI software program. Small sections of input from a MTS water example (box of water with 4 bead H atoms and 2 bead O atoms; an aqueous  $\text{Co}^{3+}$  ion with an explicit electron treated as 1024 bead ring polymer) are shown for clarity. A full set of example input files are located in the example directory on the MixPI GitHub page.

#### A. MixPI Input Files: Path-Integral Variables

A file, called rp\_molecule\_info.inp, contains information about which molecules contain atoms treated as path integrals and the number of beads for each of those atoms. The structure is as follows:

```
The number of total molecules in the simulation that contain at least one PI atom
***The following block is repeated for as many molecule types as are present ***
Number of atoms in the molecule number of molecules of this type PSF file that describes
this molecule type
    Number of beads for atom 1 in molecule
    Number of beads for atom 2 in molecule
    ...
```

In Fig. 1, we show the rp\_molecule\_info.inp file for a bulk water simulation with 90 water molecules where the O atoms are treated as 4 bead RPs and the H atoms are treated as 8 bead RPs. This file will be used by the sample make\_input.F program (which will convert classical input files to the RP input files) and the MixPI program itself.

```

90      90      SPCFw.psf      !total number of molecules with PI
3      2      !number of atoms in molecule type 1      number of molecules of type 1      the PSF file
      4      !number of beads on atom 1, molecule 1
      4      !number of beads on atom 2, molecule 1
      4      !number of beads on atom 3, molecule 1 ...

```

FIG. 1: The `rp_molecule_info.inp` file for a simulation of 90 water molecules described by the `SPCFw.psf` file with 4 bead RPs for the oxygen atoms and 8 bead RPs for the hydrogen atoms.

## B. CP2K Input Files

A set of CP2K input files, similar to those needed for a traditional CP2K MD simulation, are required. While the input structures are close to those used by classical MD, the MixPI CP2K input does need to be modified to reflect the new force and structure information for the path-integral set-ups. A simple program (called `make_input.F` which is located within the `examples/generate-input` directory) will take the classical inputs and convert them into MixPI inputs. Each of the input files is outlined in a section below.

### 1. *cp2k.inp*

The CP2K input only needs those input parameters dedicated to the force evaluations; any parameters concerning the molecular dynamics steps (like temperature, time step, etc.) are read in from a different file. The force definitions used in `cp2k.inp` must describe the interactions between the classical atoms and RP beads, the RP beads on separate atoms, and the classical atom interactions. For example, a Lennard Jones interaction of the form

$$V_{\text{LJ}} = 4\epsilon_{\text{OO}} \left[ \left( \frac{\sigma_{\text{OO}}}{r_{\text{OO}}} \right)^{12} - \left( \frac{\sigma_{\text{OO}}}{r_{\text{OO}}} \right)^6 \right] \quad (1)$$

which describes the interactions between the oxygen atoms of two water molecules has the form shown in Fig. 2. As indicated, the overall strength of the interaction ( $\epsilon_{\text{OO}}$ ) is divided by the number of beads ( $N = 2$ ) to account for the ring polymer bead interactions.

A similar force scaling is also done for the bonded interactions as well as the electrostatics.

```

&LENNARD-JONES
  ATOMS OW      OW
  EPSILON [K_e]      78.2654000000000000
  SIGMA [angstrom]   3.1654920000000000
  RCUT [angstrom]    7.0000000000000000
&END LENNARD-JONES

```

(a) The Lennard Jones parameters between two oxygen atoms in a classical simulation using the qSPC/E force-field.

```

&LENNARD-JONES
  ATOMS 2OW      2OW
  EPSILON [K_e]      39.1327000000000000
  SIGMA [angstrom]   3.1654920000000000
  RCUT [angstrom]    7.0000000000000000
&END LENNARD-JONES

```

(b) The Lennard Jones parameters between the beads of two oxygen atoms that are represented by 2 bead ring polymers using the qSPC/E force-field.

FIG. 2: The CP2K nonbonded force section between the oxygen atoms in a water simulation for the (a) classical and (b) ring polymer simulations.

## 2. *structure.psf*

A PSF file (protein structure file) is used to indicate the atom types and bonded information for the system. A psf file for "classical" qSPC/E water is shown in Fig. 3. The first block contains the atom information. The order of the columns is: atom ID, segment name, residue ID, residue name, atom name, atom type, charge, mass, and an unused 0. As we will see below, the important columns are segment name, atom name, atom type (which, when you compare to Fig. 2, matches the force-field information), charge, and mass.

## IV. THEORY

In this section, we will first review the theory behind PIMD and MTS-PIMD; similar derivations have been presented previously <sup>2,3</sup>.

```

PSF EXT

1 !SPCFw
CP2K PSF File for qSPC/E water molecule

3 !NATOM
1 MOL1      1      SOL      OW      OW      -0.840000      15.999      0
2 MOL1      1      SOL      HW      HW      0.420000      1.008      0
3 MOL1      1      Sol      HW      HW      0.420000      1.008      0

2 !NBOND
1          2          1          3

1 !NTHETA
2          1          3

0 !NPHI

0 !NIMPHI

0 !NDON

0 !NACC

0 !NNB

```

FIG. 3: The PSF file for qSPC/E water.

### 1. All Replica Ring Polymer Hamiltonian

The quantum mechanical canonical partition function can be written as

$$\begin{aligned}
Z &= \text{Tr}[e^{-\beta\hat{H}}] \\
&= \int dq \langle q | e^{-\beta\hat{H}} | q \rangle,
\end{aligned} \tag{2}$$

where  $|q\rangle$  is a position eigenstate of the one-dimensional Hamiltonian

$$\hat{H} = T(\hat{p}) + V(\hat{q}). \tag{3}$$

We use the asymmetric Trotter approximation to split the Hamiltonian into a potential and kinetic components and insert N-1 copies of the identity in the position basis ( $\hat{I} = \int dq |q\rangle \langle q|$ ) between the two components. We evaluate the potential

$$Z = \lim_{N \rightarrow \infty} \int d\{\mathbf{q}\} \prod_{\alpha=1}^N \langle q_{\alpha} | \left( e^{-\frac{\beta}{N}V(\{\hat{q}\})} e^{-\frac{\beta}{N}T(\{\hat{p}\})} \right) | q_{\alpha+1} \rangle, \tag{4}$$

where  $q_{N+1} = q_1$  to maintain the trace.

The potential and kinetic terms are evaluated with respect to the position basis.

$$Z = \lim_{N \rightarrow \infty} \left( \frac{mN}{2\pi\beta\hbar^2} \right)^{\frac{N}{2}} \int d\{\mathbf{q}\} e^{-\beta \sum_{\alpha=1}^N \left( \frac{1}{N}V(q_{\alpha}) - \frac{Nm}{2\beta^2\hbar^2}(q_{\alpha} - q_{\alpha+1})^2 \right)} \tag{5}$$



By introducing identity via a Gaussian integral over momentum divided by itself, we can rewrite the expression above as

$$Z = \lim_{N \rightarrow \infty} \left( \frac{\beta}{2\pi m_f} \right)^{1/2} \left( \frac{mN}{2\pi\beta\hbar^2} \right)^{\frac{N}{2}} \int d\{\mathbf{q}\} e^{-\beta \sum_{\alpha=1}^N \left( \frac{p_\alpha^2}{2m_f} + \frac{1}{N} V(q_\alpha) - \frac{Nm}{2\beta^2\hbar^2} (q_\alpha - q_{\alpha+1})^2 \right)} \quad (6)$$

We now have an expression in which the exponential looks similar to a classical Hamiltonian of the form

$$H_{\text{RP}} = \sum_{\alpha=1}^N \frac{p_\alpha^2}{2m_f} + \frac{1}{N} V(q_\alpha) + \frac{Nm}{2\beta^2\hbar^2} (q_\alpha - q_{\alpha+1})^2 \quad (7)$$

which is referred to as the one-dimensional PIMD Hamiltonian. For equilibrium properties, one can choose any quantity as  $m_f$ , the fictitious mass. As discussed later, this choice of  $m_f$  can improve the sampling efficiency of PIMD. This Hamiltonian can be easily expanded to multiple degrees of freedom.

### A. MTS-Expansion in Three-Dimensions

Using a similar methodology as described above, we derive the MTS-PIMD Hamiltonian below. We choose to derive the Hamiltonian for three particles in one-dimension to highlight the form of the Hamiltonian used with multiple quantization levels that the MTS-PIMD Hamiltonian can accommodate. This Hamiltonian can easily be extended to handle an arbitrary number of degrees. The quantum Hamiltonian operator for three particles is written

$$\begin{aligned} \hat{H} &= \sum_{i=1}^3 \frac{\hat{p}_i}{2m_i} + \sum_{i=1}^3 V_1(\hat{q}_i) + \sum_{i=1}^3 \sum_{j<i} V_2(\hat{q}_i, \hat{q}_j) + \sum_{i=1}^3 \sum_{j<i} \sum_{k<j} V_3(\hat{q}_i, \hat{q}_j, \hat{q}_k) \\ &= H_1(\hat{q}_1, \hat{q}_2, \hat{q}_3) + H_2(\hat{q}_2, \hat{q}_3) + H_3(\hat{q}_3) \end{aligned} \quad (8)$$

where  $\hat{p}_i$ ,  $\hat{q}_j$ , and  $m_i$  are the momentum, position, and mass of the  $i^{\text{th}}$  quantum particle.  $V_1(\hat{q}_i)$  is the uncoupled portion of the potential energy for the  $i^{\text{th}}$  degree while  $V_2(\hat{q}_i, \hat{q}_j)$  and  $V_3(\hat{q}_i, \hat{q}_j, \hat{q}_k)$  are the two-body and three-body coupled potential energy contributions, respectively. We assume that the  $q_1$  degree of freedom experiences the largest quantum mechanical effect, followed by  $q_2$  and then  $q_3$ ; therefore,  $q_1$  requires more time slices, and a larger  $N$  value, than  $q_2$ . We define  $N_1$ ,  $N_2$ , and  $N_3$  as the number of time slices along each degree with  $N_1 \geq N_2 \geq N_3$ . We split the Hamiltonian by dependence on particle number where any two- or three-body terms are included in the Hamiltonian corresponding to the highest quantized

variable. For example,  $H_1(\hat{q}_1, \hat{q}_2, \hat{q}_3) = T_1(\hat{p}_1) + V(\hat{q}_1) + V(\hat{q}_1, \hat{q}_2) + V(\hat{q}_1, \hat{q}_3) + V(\hat{q}_1, \hat{q}_2, \hat{q}_3)$ . As describe in Sec. IV 1, we use the asymmetric Trotter approximation on this partitioned Hamiltonian to first split  $H_3$  from  $H_{12}$

$$Z = \lim_{N_3 \rightarrow \infty} \int d\{q\} \langle q_1 q_2 q_3 | \left( e^{-\frac{\beta H_3}{N_3}} e^{-\frac{\beta H_{12}}{N_3}} \right)^{N_3} | q_1 q_2 q_3 \rangle \quad (9)$$

and then apply the Trotter approximation twice more to  $H_{12} = H_1 + H_2$  and, finally, to  $H_1$  to obtain

$$Z = \lim_{N_3, N_2, N_1 \rightarrow \infty} \int d\{q\} \langle q_1 q_2 q_3 | \left( \Lambda_3 (\Lambda_{21})^{\frac{N_2}{N_3}} \right)^{N_3} | q_1 q_2 q_3 \rangle. \quad (10)$$

where we define  $\Lambda_i = e^{-\frac{\beta H_i}{N_i}}$  and  $\Lambda_{ij} = \Lambda_i \Lambda_j^{\frac{N_j}{N_i}}$ . Following a similar series of steps as employed in the all-replica derivation in the previous section, we insert  $N_3$  copies of identity with respect to the position basis  $q_3$  and evaluate  $\Lambda_{12}$  since it is diagonal with respect to  $q_3$ .

$$Z = \lim_{N_3, N_2, N_1 \rightarrow \infty} \int d\{q\} \langle q_1 q_2 | \prod_{\alpha=1}^{N_3} \langle q_{3,\alpha} | \Lambda_3 | q_{3,\alpha+1} \rangle \Lambda_{12}(q_{3,\alpha+1})^{\frac{N_2}{N_3}} | q_1 q_2 \rangle. \quad (11)$$

We now have the one-particle results with  $H_3$  and can use the result of the previous derivation to obtain

$$\begin{aligned} Z = \lim_{N_3, N_2, N_1 \rightarrow \infty} & \left( \frac{\beta}{2\pi m_{3,f}} \right)^{1/2} \left( \frac{m_3 N_3}{2\pi \beta \hbar^2} \right)^{\frac{N_3}{2}} \\ & \int d\{q\} e^{-\beta \sum_{\alpha=1}^{N_3} \left( \frac{p_{3,\alpha}^2}{2m_{3,f}} + \frac{1}{N_3} V_1(q_{3,\alpha}) - \frac{N_3 m_3}{2\beta^2 \hbar^2} (q_{3,\alpha} - q_{3,\alpha+1})^2 \right)} \\ & \langle q_1 q_2 | \prod_{\alpha=1}^{N_3} \Lambda_{12}(q_{3,\alpha+1})^{\frac{N_2}{N_3}} | q_1 q_2 \rangle. \end{aligned} \quad (12)$$

Next, we introduce  $N_3$  copies of identity with respect to  $q_2$  between each of the  $\Lambda(q_{3,\alpha+1})^{N_2/N_3}$  terms

$$\begin{aligned} Z = \lim_{N_3, N_2, N_1 \rightarrow \infty} & A_3 \int d\{q\} e^{-\beta H_{3,RP}(q_3)} \\ & \langle q_1 | \prod_{\alpha=1}^{N_3} \langle q_{2,(\alpha-1)*N_2/N_3+1} | \Lambda_{12}(q_{3,\alpha+1})^{\frac{N_2}{N_3}} | q_{2,\alpha*N_2/N_3+1} \rangle | q_1 \rangle. \end{aligned} \quad (13)$$

Since  $q_2$  is more quantized than  $q_3$ , and needs a greater number of slices than  $q_3$ , we introduce

additional  $N_2/N_3$  copies of identity between each  $\Lambda_{12}(q_{3,\alpha+1})$

$$Z = \lim_{N_3, N_2, N_1 \rightarrow \infty} A_3 \int d\{q\} e^{-\beta H_{3,RP}(q_3)} \langle q_1 | \prod_{\alpha=1}^{N_3} \prod_{\gamma=1}^{N_2/N_3} \langle q_{2,(\alpha-1)*N_2/N_3+\gamma} | \Lambda_2(q_{3,\alpha+1}) \Lambda_1(q_{3,\alpha+1})^{\frac{N_1}{N_2}} | q_{2,(\alpha-1)*N_2/N_3+\gamma+1} \rangle | q_1 \rangle. \quad (14)$$

$\Lambda_1(q_{3,\alpha+1})$  is diagonal with respect to  $q_2$  and we have obtained the one-dimensional ring-polymer solution for  $q_2$ .

$$Z = \lim_{N_3, N_2, N_1 \rightarrow \infty} A_3 A_2 \int d\{q\} e^{-\beta H_{3,RP}(\{q_3\})} e^{-\beta H_{2,RP}(\{q_2\}, \{q_3\})} \prod_{\alpha=1}^{N_3} \prod_{\gamma=1}^{N_2/N_3} \langle q_1 | \Lambda_1(q_{3,\alpha+1}, q_{2,(\alpha-1)*N_2/N_3+\gamma+1})^{\frac{N_1}{N_2}} | q_1 \rangle. \quad (15)$$

We follow the same procedure to introduce  $N_2$  copies of identity between each  $\Lambda_1(q_{3,\alpha+1}, q_{2,(\alpha-1)*N_2/N_3+\gamma+1})^{\frac{N_1}{N_2}}$  and  $N_1/N_2$  copies of identity between each  $\Lambda_1(q_{3,\alpha+1}, q_{2,(\alpha-1)*N_2/N_3+\gamma+1})$  to obtain the all-replica Hamiltonian for  $q_1$ . We obtain an expression for the three-level mixed-time slicing RPMD partition function and Hamiltonian

$$Z = \lim_{N_3, N_2, N_1 \rightarrow \infty} A_3 A_2 A_1 \int d\{q\} e^{-\beta H_{3,RP}(\{q_3\})} e^{-\beta H_{2,RP}(\{q_2\}, \{q_3\})} e^{-\beta H_{1,RP}(\{q_1\}, \{q_2\}, \{q_3\})}. \quad (16)$$

where

$$\begin{aligned} H_{3,RP} &= \sum_{\alpha=1}^{N_3} \frac{p_{3,\alpha}^2}{2m_{3,f}} + \frac{1}{N_3} V_1(q_{3,\alpha}) - \frac{N_3 m_3}{2\beta^2 \hbar^2} (q_{3,\alpha} - q_{3,\alpha+1})^2 \\ H_{2,RP} &= \sum_{\alpha=1}^{N_3} \sum_{\gamma=1}^{N_2/N_3} \frac{p_{2,(\alpha-1)*N_2/N_3+\gamma}^2}{2m_2} + \frac{1}{N_2} V_1(q_{2,(\alpha-1)*N_2/N_3+\gamma}) + \frac{1}{N_2} V_2(q_{2,(\alpha-1)*N_2/N_3+\gamma}, q_{3,\alpha}) \\ &\quad + \frac{N_2 m_2}{2\beta^2 \hbar^2} (q_{2,(\alpha-1)*N_2/N_3+\gamma} - q_{2,(\alpha-1)*N_2/N_3+\gamma+1})^2 \\ H_{1,RP} &= \sum_{\alpha=1}^{N_3} \sum_{\gamma=1}^{N_2/N_3} \sum_{\lambda=1}^{N_1/N_2} \frac{p_{1,((\alpha-1)*N_2/N_3+\gamma-1)*N_1/N_2+\lambda}^2}{2m_1} + \frac{1}{N_1} V_1(q_{1,((\alpha-1)*N_2/N_3+\gamma-1)*N_1/N_2+\lambda}) \\ &\quad + \frac{1}{N_1} V_2(q_{1,((\alpha-1)*N_2/N_3+\gamma-1)*N_1/N_2+\lambda}, q_{2,(\alpha-1)*N_2/N_3+\gamma}) \\ &\quad + \frac{1}{N_1} V_2(q_{1,((\alpha-1)*N_2/N_3+\gamma-1)*N_1/N_2+\lambda}, q_{3,\alpha}) \\ &\quad + \frac{1}{N_1} V_3(q_{1,((\alpha-1)*N_2/N_3+\gamma-1)*N_1/N_2+\lambda}, q_{2,(\alpha-1)*N_2/N_3+\gamma}, q_{3,\alpha}) \\ &\quad + \frac{N_3 m_3}{2\beta^2 \hbar^2} (q_{1,((\alpha-1)*N_2/N_3+\gamma-1)*N_1/N_2+\lambda} - q_{1,((\alpha-1)*N_2/N_3+\gamma-1)*N_1/N_2+\lambda+1})^2 \end{aligned} \quad (17)$$

As shown in the above derivation, the splitting of different components of a system into different quantization levels follows a similar methodology to the standard all-replica methodology. While the resulting Hamiltonian expression is slightly more complex, it allows for a significant reduction in the computational time and resources necessary to conduct PIMD and RPMD simulations. By allowing different levels of quantization, we decrease the overall number of particles in the system. While this has some advantages with respect to propagation of the position and momentum variables, as well as the intra-ring polymer spring forces, the most intensive savings occurs during the force-evaluations. By decreasing the number of force evaluations required, the computation time for each molecular dynamics step is significantly faster.

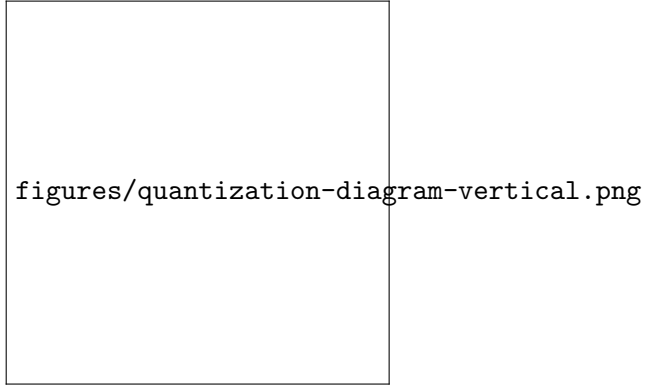


FIG. 4: A diagram showing the different forces between ring polymers at four different quantization schemes: (a) all classical, (b) all quantum, (c) quantum-classical, and (d) mixed-time slicing.

In Fig. 5, we show the number of individual two-body forces calculated between two particles at different quantization schemes. In Fig. 5a, the single "classical" force is evaluated between two particles ( $V_2(q_1, q_2)$ ). In Equation 17, the two-particle potential between particle 1 and particle 2 is

$$\sum_{\gamma=1}^{N_2} \sum_{\lambda=1}^{N_1/N_2} \frac{1}{N_1} V_2(q_{1,(\gamma-1)*N_1/N_2+\lambda}, q_{2,\gamma})$$

. If  $N_1 = N_2$ , as in Fig 5b, the potential is simplified to  $\sum_{\gamma=1}^{N_1} \frac{1}{N_1} V_2(q_{1,\gamma}, q_{2,\gamma})$ . This is the standard ring polymer scheme where each bead only experiences a force from the same bead replica on the other particle. In this example, bead 1 on particle 1 only experiences an inter-PI force from bead 1 on particle 2. This force is one-fourth the magnitude of the force between the two classical particles since  $N_1 = 4$ .

figures\_SI/quantization-diagram-3atoms.pdf

FIG. 5: A diagram showing the different forces between ring polymers at four different quantization schemes: (a) all classical, (b) all quantum, (c) quantum-classical, and (d) mixed-time slicing.

Using the same expression, we can evaluate what happens when there are unequal number of beads on the two particles. In the simplest case, one particle is treated classically as shown in Fig. 5c, and  $N_2 = 1$ . In this case, the two particle potential simplifies to  $\sum_{\lambda=1}^{N_1} \frac{1}{N_1} V_2(q_{1,\lambda}, q_{2,1})$ . In the more complicated MTS example shown in Fig. 5d, where  $N_1 = 4$  and  $N_2 = 2$ , the expression for the inter-PI force becomes  $\sum_{\gamma=1}^{N_2} \sum_{\lambda=1}^2 \frac{1}{N_1} V_2(q_{1,(\gamma-1)2+\lambda}, q_{2,\gamma})$ . Since ratios for different  $N_\alpha$  values appear in the indexing for the interaction terms, MixPI requires that all  $N_\alpha$  values be powers of 2.

Each two-body force or potential energy evaluation in Fig. 5b-d requires four separate evaluations. In general, any multi-body force or energy calculation requires  $N_{\max}$  number of individual force or energy evaluations. Therefore, when using potentials that contain all-body terms, like those in DFT-based methods, the all-replica results and the MTS results will have similar computational expenditures. This scaling is why the MTS-RPMD method is most appropriate for methods that utilize additive force-fields and energy schemes. In

the implementation section below, we will discuss in more detail the relative computational costs of MTS-RPMD versus other implementations.

In the two systems discussed below, we utilized the smooth-particle mesh Ewald routine in CP2K to analyze the long range, periodic electrostatic energies and forces<sup>4</sup>. This routine utilizes a many-body expression for the electrostatic energy. Since the electrostatic forces are smoothly varying, we approximate the energies and forces between path-integral beads to be the forces between the centroids. A similar approximation has been used in previous PI techniques, such as ring polymer contraction methods<sup>5–7</sup>, and has been shown to return approximate forces and energies that are in close agreement with the exact PI results. The use of centroid force approximations, along with other approximate force treatments, will be explored in future work to expand the applicability of MTS-RPMD beyond force-field treatments.

## REFERENCES

- <sup>1</sup>T. D. Kühne, M. Iannuzzi, M. Del Ben, V. V. Rybkin, P. Seewald, F. Stein, T. Laino, R. Z. Khaliullin, O. Schütt, F. Schiffmann, D. Golze, J. Wilhelm, S. Chulkov, M. H. Bani-Hashemian, V. Weber, U. Borštnik, M. TAILLEFUMIER, A. S. Jakobovits, A. Lazzaro, H. Pabst, T. Müller, R. Schade, M. Guidon, S. Andermatt, N. Holmberg, G. K. Schenter, A. Hehn, A. Bussy, F. Belleflamme, G. Tabacchi, A. Glöß, M. Lass, I. Bethune, C. J. Mundy, C. Plessl, M. Watkins, J. VandeVondele, M. Krack, and J. Hutter, “Cp2k: An electronic structure and molecular dynamics software package - quickstep: Efficient and accurate electronic structure calculations,” *The Journal of Chemical Physics* **152** (2020), 10.1063/5.0007045.
- <sup>2</sup>R. P. Steele, J. Zwickl, P. Shushkov, and J. C. Tully, “Mixed time slicing in path integral simulations,” *The Journal of Chemical Physics* **134** (2011), 10.1063/1.3518714.
- <sup>3</sup>M. Ceriotti, M. Parrinello, T. E. Markland, and D. E. Manolopoulos, “Efficient stochastic thermostating of path integral molecular dynamics,” *The Journal of Chemical Physics* **133** (2010), 10.1063/1.3489925.
- <sup>4</sup>U. Essmann, L. Perera, M. L. Berkowitz, T. Darden, H. Lee, and L. G. Pedersen, “A smooth particle mesh ewald method,” *The Journal of Chemical Physics* **103**, 8577–8593 (1995).

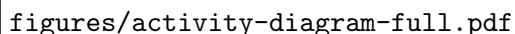
The figure is an activity diagram for the MTS-RPMD software program. It is a rectangular box containing the text 'figures/activity-diagram-full.pdf'. The diagram is partitioned into lanes to indicate the input and output files created and accessed by the user (labelled USER on left), the procedure followed by the MTS-RPMD program as it proceeds through the molecular dynamics steps (labelled MTS-RPMD PROGRAM in center) and the subsequent locations where it accesses the force and energy evaluation subroutines in CP2K (labelled CP2K on right).

FIG. 6: An activity diagram that outlines the procedure followed by the MTS-RPMD software program. The activity diagram is partitioned into lanes to indicate the input and output files created and accessed by the user (labelled USER on left), the procedure followed by the MTS-RPMD program as it proceeds through the molecular dynamics steps (labelled MTS-RPMD PROGRAM in center) and the subsequent locations where it accesses the force and energy evaluation subroutines in CP2K (labelled CP2K on right).

<sup>5</sup>T. E. Markland and D. E. Manolopoulos, “An efficient ring polymer contraction scheme for imaginary time path integral simulations,” *The Journal of Chemical Physics* **129** (2008), 10.1063/1.2953308.

<sup>6</sup>O. Marsalek and T. E. Markland, “Ab initio molecular dynamics with nuclear quantum effects at classical cost: Ring polymer contraction for density functional theory,” *The Journal*

of Chemical Physics **144** (2016), 10.1063/1.4941093.

<sup>7</sup>V. Kapil, J. VandeVondele, and M. Ceriotti, “Accurate molecular dynamics and nuclear quantum effects at low cost by multiple steps in real and imaginary time: Using density functional theory to accelerate wavefunction methods,” The Journal of Chemical Physics **144** (2016), 10.1063/1.4941091.